

## Dielectric spectroscopy of glass-forming materials: $\alpha$ -relaxation and excess wing

Peter Lunkenheimer, Alois Loidl

### Angaben zur Veröffentlichung / Publication details:

Lunkenheimer, Peter, and Alois Loidl. 2002. "Dielectric spectroscopy of glass-forming materials:  $\alpha$ -relaxation and excess wing." *Chemical Physics* 284 (1-2): 205–19.  
[https://doi.org/10.1016/S0301-0104\(02\)00549-9](https://doi.org/10.1016/S0301-0104(02)00549-9).

# Dielectric spectroscopy of glass-forming materials: $\alpha$ -relaxation and excess wing

P. Lunkenheimer\*, A. Loidl

*Universität Augsburg, Universitätsstr. 2, D-86135 Augsburg, Germany*

## 1. Introduction

Since about 200 years, starting with the pioneering work of Fraunhofer, non-crystalline materials are an object of scientific investigation and a lot has been learned about the glassy state of matter in this time. However, one has to state that we are still far from a thorough microscopic understanding of the rich phenomenology of glassy systems and while a variety of different theoretical approaches has appeared, by no means a general

accord has been reached. Maybe the most challenging task is to understand the microscopic dynamics underlying the glass transition, with its tremendous, yet continuous slow down of molecular kinetics when a liquid transforms into a glass. During recent years, dielectric spectroscopy has proven an important technique for the investigation of this dynamics and dielectric investigations of glass-forming liquids have contributed significantly to our understanding of the glass transition [e.g., 1–13]. The exceptionally broad time/frequency window, accessible with this method, makes it an ideal tool to follow the many decade change of molecular kinetics at the glass transition. Moreover, as we have learned due to the experimental progress of recent years, glass-forming materials show a rich variety of dynamic pro-

---

\*Corresponding author. Tel.: +49-821-598-3603; fax: +49-821-598-3649.

E-mail address: [peter.lunkenheimer@physik.uni-augsburg.de](mailto:peter.lunkenheimer@physik.uni-augsburg.de) (P. Lunkenheimer).

cesses in addition to the structural  $\alpha$ -relaxation, which determines, e.g., the viscosity. These additional contributions, like high-frequency wing or boson peak, have attracted considerable interest in recent years and the understanding of their microscopic origin is often considered as a prerequisite for a thorough understanding of the glass transition and glass state. All these processes can be investigated by broadband dielectric spectroscopy. In order to achieve a coupling of the molecular kinetics to the probing field, the experiments are typically performed either on non-conducting dipolar or on ionically conducting glass-forming liquids. Usually materials with simple molecular structure, high glass-forming ability, and the glass temperature  $T_g$  in a convenient temperature range are chosen. In the present work we will show results on some prototypical materials, obtained in an exceptionally broad frequency range. Thereby we will give an overview of the typical glassy dynamic behavior showing up in dielectric spectroscopy. Especially we will concentrate on the  $\alpha$ -relaxation and its phenomenology and on the so-called excess wing, which shows up as an excess contribution at frequencies beyond the  $\alpha$ -relaxation and whose true origin has been revealed only recently [12].

## 2. Glassy kinetics revealed by dielectric spectroscopy

Fig. 1 schematically depicts the typical broadband dielectric loss spectra of non-conducting glass-forming materials, demonstrating the most common contributions from different dynamic processes for two prototypical cases [13,14]. In most dielectric experiments, essentially the reorientational dynamics of dipolar molecules, coupling to the structural rearrangement processes is detected. The  $\alpha$ -process then leads to a dominant loss peak at  $\nu_p \approx \nu_\tau = 1/(2\pi\langle\tau_\alpha\rangle)$ , with  $\langle\tau_\alpha\rangle$  the average  $\alpha$ -relaxation time. Fig. 1 shows the situation near  $T_g$ , with the  $\alpha$ -peak situated at a rather low frequency. With increasing temperature it will rapidly shift to higher frequencies. For most glass formers the loss peaks are broader than expected from Debye theory, which presumes an exponen-

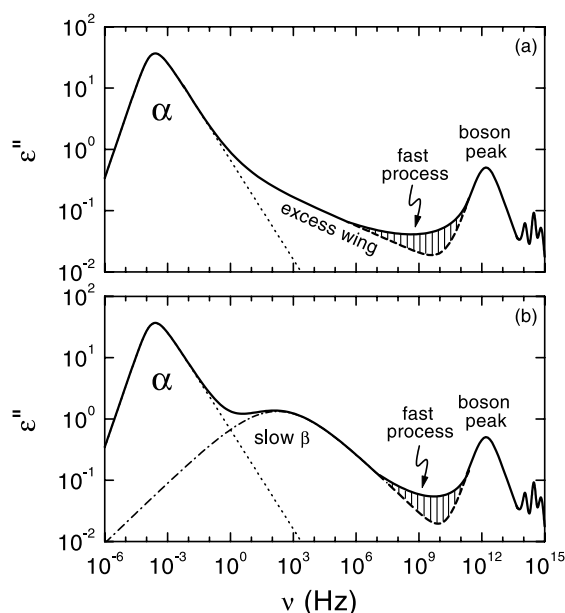


Fig. 1. Schematic view of the frequency-dependent dielectric loss in non-conducting glass-forming materials as observed in extremely broadband measurements [13,14]. Two typical cases are shown, namely the response of glass-formers showing an excess wing (a) and of glass-formers with a well-resolved  $\beta$ -relaxation peak (b). The contribution of an additional fast process in the minimum region preceding the boson peak is indicated by the hatched area.

tial time-dependence of the  $\alpha$ -relaxation process. This finding is commonly ascribed to a distribution of relaxation times, caused by variations of the local environment of the relaxing entities [15]. In addition,  $\tau_\alpha(T)$  usually deviates significantly from Arrhenius behavior. The temperature dependence of  $\tau_\alpha$  is one of the most important informations concerning the dynamics of glass-forming materials and can be evaluated within various theoretical and phenomenological frameworks.

If mobile charge carriers are present, conductivity contributions lead to a divergence of the loss  $\varepsilon''(\nu)$  for low frequencies, as  $\varepsilon'' \sim \sigma'/\nu$ , with  $\sigma'$  the real part of the conductivity. Conductivity contributions are not shown in Fig. 1, i.e. the situation for a completely insulating glass former is depicted. For ionically conducting glass formers the conductivity contribution becomes dominant and can completely suppress the other features in the

spectra (if present). In these materials the conductivity directly reflects the translational kinetics of the molecules, which is closely linked to the  $\alpha$ -relaxation. Indeed for many ionically conducting glass-forming liquids the temperature dependence of the dc conductivity parallels that of the  $\alpha$ -relaxation time, at least at high temperatures. Dielectric results on ionically conducting materials often are represented in terms of the frequency-dependent complex conductivity and analyzed within theoretical models for hopping conductivity of ionic charge carriers (e.g., [16,17]). But for ionically conducting glass-formers also a completely different approach is often used: In [18] a variety of arguments were put forward in favor of the employment of the dielectric modulus,  $M^* = 1/\varepsilon^*$  ( $\varepsilon^*$  the complex dielectric permittivity), to gain information on the  $\alpha$ -relaxation process in ionically conducting glass-formers. The spectra of the imaginary part  $M''(\nu)$  reveal quite a similar behavior as  $\varepsilon''(\nu)$  of non-conducting glass formers, namely a peak whose properties resemble those of the  $\alpha$ -peak observed in  $\varepsilon''(\nu)$ . From the position of the modulus peak the so-called conductivity relaxation time  $\tau_\sigma$  can be determined, which is believed to be a characteristic time for molecular motion in ionically conducting glass formers and indeed, at least for high temperatures, often is found to follow the  $\alpha$ -relaxation time determined by other methods. However, it has to be mentioned that there is an ongoing controversy concerning the physical meaning of this representation (see, e.g., [19]). Also one has to be aware that in most ionically conducting glass-formers, at lower temperatures the ionic motion becomes increasingly decoupled from the structural relaxation processes. In this regime the conductivity relaxation time deviates markedly from the structural  $\alpha$ -relaxation time.

In addition to the  $\alpha$ -relaxation, a variety of other features show up in broadband dielectric spectra of supercooled materials. At frequencies some decades above  $\nu_p$  in many glass-formers an excess contribution to the high-frequency flank of the  $\alpha$ -peak is observed (Fig. 1(a)) [3,6,20–22]. This “excess wing” can be reasonably well described by a second power law,  $\varepsilon'' \sim \nu^{-b}$  with  $b < \beta$ , in addition to the power law  $\nu^{-\beta}$ , commonly found at

$\nu > \nu_p$  [3,20–23]. Some theoretical explanations for its occurrence have been proposed in [24–26] and intriguing scaling properties of  $\alpha$ -peak and excess wing were reported in [6]. However, yet no consensus on the microscopic origin of this phenomenon has been reached.

In many glass-forming materials, a slow  $\beta$ -relaxation shows up as indicated in Fig. 1(b). Sometimes intramolecular motions are held responsible for  $\beta$ -relaxations, but Johari and Goldstein [2,27] demonstrated that secondary relaxation processes also show up in relatively simple molecular glass-formers, where intramolecular contributions seem unlikely. This led to the notion that these so-called Johari–Goldstein  $\beta$ -relaxations may be inherent to glass-forming materials in general [2,27]. However, the microscopic processes behind this kind of  $\beta$ -relaxations are still controversially discussed. Until recently, it was commonly assumed that the excess wing and the Johari–Goldstein  $\beta$ -relaxations are due to different processes [6,28] and even the existence of two classes of glass-formers was suggested [28] – “type A” without a  $\beta$ -process but showing an excess wing (corresponding to Fig. 1(a)) and “type B” with a  $\beta$ -process (Fig. 1(b)) [29]. However, it also seems possible that excess wing and  $\beta$ -relaxation are due to the same microscopic process as considered in several publications [3,30–35]. Indeed recently some strong experimental hints have emerged that the excess wing is simply the high-frequency flank of a  $\beta$ -peak, hidden under the dominating  $\alpha$ -peak [12].

At some THz a further loss-peak shows up that can be identified with the so-called boson peak known from neutron and light scattering (see, e.g., [36]). The boson peak is a general feature of glass-forming materials and corresponds to the commonly found excess contribution in specific heat measurements at low temperatures and a variety of theoretical explanations have been proposed, to account for its occurrence.

Between the  $\alpha$ -peak and the boson peak, obviously a minimum in  $\varepsilon''(\nu)$  must exist, corroborated by the findings in a variety of scattering experiments. Until recently, the relevant frequency region of about 10–100 GHz laid just at the high-frequency edge of the range available even in very

well-equipped dielectric laboratories (but, see, e.g., [4,5]). However, recent experimental advances enabled to obtain continuous dielectric spectra on glass-forming materials extending well into the relevant region [10,11,13,37]. In accordance with light and neutron scattering results (e.g., [36]), these high-frequency measurements reveal the presence of a fast process, sometimes termed “fast  $\beta$ -process”, as indicated by the hatched area in Fig. 1 [10,11,13,35,37]. Contributions from a fast process in this spectral region were predicted by the mode coupling theory (MCT) of the glass transition [38,39], which currently is the most promising, but also most controversially discussed theoretical approach of the glass transition. In MCT the fast process can be roughly ascribed to the “rattling” movement of a particle in the transient “cage” formed by its neighbors. Also other explanations of these fast contributions may be possible (e.g., [25]). Finally, in the infrared region various resonance-like features can be expected which are due to phonon-like modes and vibrational and rotational excitations of the molecules.

### 3. Experimental

To record the real and imaginary parts of the dielectric permittivity in a broad frequency range, the combination of a variety of different techniques is necessary. In general, at low frequencies,  $\nu \leq 2$  GHz, the samples are prepared in parallel-plate capacitor geometry. Up to several 10 MHz, essentially the capacitance and conductance of the sample are measured directly. In this region time-domain techniques [40], frequency response analysis, and autobalance bridges are used. Between 1 MHz and about 10 GHz, the coaxial reflection method is most appropriate. Here the sample is connected to the end of a coaxial line, thereby bridging inner and outer conductors [41]. The devices (impedance or network analyzers) measure the complex reflection coefficient or perform a direct current–voltage measurement. At frequencies up to 30 GHz measurements are taken in transmission geometry: A network analyzer measures the transmission properties of a coaxial line, filled with the sample material.

The region between some 10 and some 100 GHz is difficult to access and therefore only rarely investigated. Here the free-space technique can be used where the electromagnetic wave, generated by a monochromatic source, propagates through “free space” (i.e., is unguided) and is detected by a suitable detector after passing (or being reflected by) the sample. In principle, setups as known from optical spectrometers can be applied. The Mach–Zehnder interferometer [42] allows to measure the frequency dependence of both, the transmission and the phase shift, of a monochromatic electromagnetic beam through the sample. The frequency range up to 1.2 THz is covered continuously by 10 tunable narrow-band backward-wave oscillators (BWOs). In the frequency region between several 100 GHz and optical frequencies, commercially available infrared spectrometers are used. Here usually the determination of the phase shift is not possible and a Kramers–Kronig transformation has to be applied to deduce the complex dielectric permittivity.

For cooling and heating of the samples, a closed cycle refrigerator, a nitrogen gas-heating system, and various ovens are used. For the aging experiments, the samples were kept at a fixed temperature for up to five weeks in the closed-cycle refrigerator system. The samples were cooled from a temperature about 20 K above  $T_g$  with the maximum possible cooling rate of about 3 K/min. The final temperature was reached without any temperature undershoot. As zero point of the aging times reported below, we took the time when the desired temperature was reached, about 200 s after passing  $T_g$ . The temperature was detected by a Platinum sensor, inserted into one capacitor plate and kept stable within 0.02 K during the measurement time of up to five weeks.

For more details on experimental setups and sample preparation the reader is referred to [12,13,41–45].

### 4. Results and discussion

#### 4.1. Dielectric spectra of glass forming materials

Fig. 2 shows spectra of the dielectric constant  $\epsilon'$  and the dielectric loss  $\epsilon''$  of glass-forming glycerol

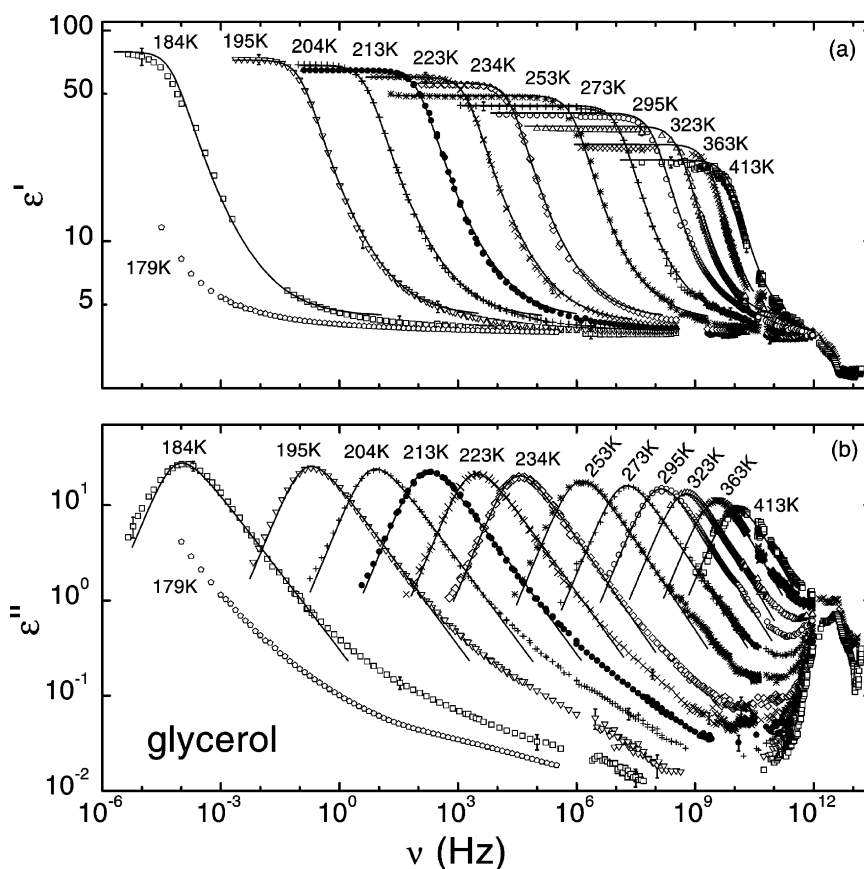


Fig. 2. Frequency dependence of the real and the imaginary parts of the dielectric permittivity in glycerol at various temperatures [10,12–14,35,45,46] (to keep the figure readable, at high frequencies not all data point are shown; especially in the THz region results are shown for two temperature only). The sub- $T_g$  curve at 179 K was measured in thermal equilibrium after five weeks aging time [12]. The lines are fits of the region near  $\nu_p$  with the CD function, performed simultaneously on  $\epsilon'$  and  $\epsilon''$ .

for various temperatures, extending over nearly 19 decades of frequency [10,12–14,45,46]. Glycerol belongs to the group of low molecular-weight organic glass-formers and due to its very low crystallization tendency and convenient glass temperature ( $T_g \approx 185$  K) is one of the most thoroughly investigated glass-forming materials. The loss spectra (Fig. 2(b)) follow the schematic behavior of Fig. 1(a). By changing the temperature by about a factor of two, the typical asymmetrically shaped  $\alpha$ -relaxation peaks shift by 14 decades of frequency. This mirrors the dramatic slowing down of the structural  $\alpha$ -dynamics during the transition from the low-viscosity liquid to the glass. The loss peaks are accompanied by relax-

ation steps in  $\epsilon'(\nu)$  as seen in Fig. 2(a). The  $\alpha$ -relaxation will be treated in more detail in the next section. At frequencies  $\nu > \nu_p$ ,  $\epsilon''(\nu)$  follows a power law  $\epsilon'' \sim \nu^{-\beta}$ . At higher frequencies deviations from this power law occur: For low temperatures,  $T \leq 253$  K, an excess wing shows up as second power law,  $\nu^{-b}$  with  $b < \beta$  before the minimum region is reached. Its slope increases with increasing temperature and at high temperatures it seems to merge with the  $\alpha$ -peak. More details on the excess wing will be given in Section 4.3.

In the GHz–THz frequency region a minimum in  $\epsilon''(\nu)$  is observed. With decreasing temperature, its amplitude and frequency position decreases and it becomes significantly broader. The minimum is

too shallow to be explained by a simple superposition of  $\alpha$ -peak/excess wing and the boson peak that shows up around THz, which clearly indicates contributions from a fast process in this region [10,13,35,47]. In earlier measurements a high-frequency minimum in  $\varepsilon''(\nu)$ , theoretically predicted by the MCT, could not be detected, mainly due to the restricted frequency range covered [3,48,49]. This even led to the conjecture that there might be no minimum at all [5,48–50]. However, the presence of this minimum in various glass-formers is now well established [10,11,13,35,37,45] and for a variety of materials it was shown that in many aspects it follows the predictions of MCT [10,11,13,35,47,51,52].

In Fig. 2(b), in the THz region of  $\varepsilon''(\nu)$  a peak shows up (to keep the figure readable, it is only shown for 184 K), a feature that is known from various earlier dielectric measurements of glass-forming materials [53]. The peak frequency is temperature independent within the experimental error; its amplitude increases weakly with temperature. Corresponding to the peak in  $\varepsilon''(\nu)$ ,  $\varepsilon'(\nu)$  exhibits a step-like decrease near 1 THz (Fig. 2(a)). For 363 K no minimum and no peak but only a shoulder is detected, due to the close vicinity of  $\alpha$ - and THz-peak. This peak is located at about the same frequency as that found in the susceptibility determined from light and neutron scattering experiments [36] and thereby can be identified with the boson peak. A more detailed discussion of the boson peak can be found in [13,14]. Finally at frequencies around 10 THz some resonance-like features appear, which mark the onset of the regime of intramolecular excitations.

To give an example of the typical dielectric response of ionically conducting glass formers, in Fig. 3(a),  $\varepsilon''(\nu)$  for  $[\text{Ca}(\text{NO}_3)_2]_{0.4}[\text{KNO}_3]_{0.6}$  (CKN,  $T_g = 333$  K) is shown for 379 K. The dielectric loss spectrum of this widely investigated material shows no indication of a  $\alpha$ -relaxation peak. Instead it is dominated by a huge increase towards low frequencies. This behavior can be ascribed to conductivity contributions from ionic transport. If, e.g., a frequency-independent conductivity,  $\sigma(\nu) = \sigma_{dc}$ , is assumed,  $\varepsilon'' \sim \sigma_{dc}/\nu$  is expected. At the lowest frequencies the high-temperature curves show a transition to a weaker frequency depen-

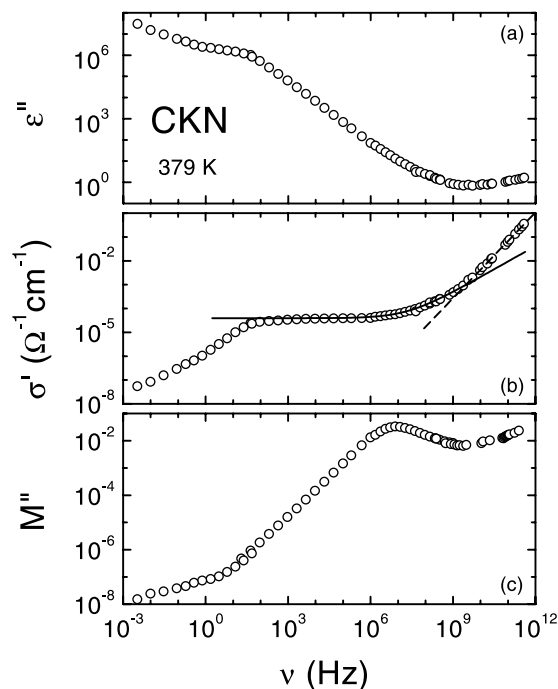


Fig. 3. Dielectric response of CKN at 379 K in three representations, namely dielectric loss (a), real part of conductivity (b), and imaginary part of dielectric modulus (c) [11,14,35,44]. The solid line in (b) is a fit of the region 100 Hz–3 GHz with the UDR [55],  $\sigma' = \sigma_{dc} + \sigma_0 \nu^s$  ( $s = 0.65$ ). The dashed line demonstrates a superlinear increase ( $\sigma' \sim \nu^{1.2}$ ) for the highest frequencies.

dence. This is a common behavior for ionic conductors and ascribed to electrode polarization effects (“blocking electrodes”) [18,54]. Only above GHz,  $\varepsilon''(\nu)$  resembles the behavior in glycerol (Fig. 2(b)) showing a rather shallow minimum (the measurements do not extend into the boson-peak region).

Such data often are analyzed in terms of the conductivity,  $\sigma' \sim \varepsilon''/\nu$ , as demonstrated in Fig. 3(b). Here the solid line is a fit of the region up to 1 GHz using the so-called Universal Dielectric Response (UDR) ansatz [55]:  $\sigma' = \sigma_{dc} + \sigma_0 \nu^s$ ,  $s < 1$ . The sublinear  $\nu^s$  power law is often ascribed to hopping conduction of localized charge carriers and there are various theoretical models of ionic conductivity predicting an approximate  $\nu^s$  behavior (e.g., [16,17]). Above GHz frequencies, deviations of fit and experimental data show up and a

slightly superlinear increase is approached, indicated by the dashed line. Such a behavior is also often observed in ionically conducting materials and was termed “second universality” or “nearly constant loss” (e.g., [56]). However, the development of a microscopic understanding of this phenomenon is still in its beginning stages.

As mentioned in Section 2, a completely different way of analysis is given by the modulus formalism [18]. In Fig. 3(c) the imaginary part of the dielectric modulus  $M''$  is shown for CKN at 379 K. It shows a peak, closely resembling the  $\alpha$ -peak in the dielectric loss of non-conducting glass-formers. Electrode polarization leads to small deviations at  $\nu \ll 1/(2\pi\tau)$  and very low values of  $M''$  only. Also in  $M''(\nu)$  a minimum at high frequencies is observed.

It certainly is a unsatisfying situation that dielectric results on ionically conducting glass formers are treated in literature according to quite different approaches: the conductivity representation is usually preferred by scientists interested mainly in ionic hopping conductivity and the modulus formalism is mainly used by those interested in glassy dynamics. Here we cannot solve this ambiguity, but at least it may be mentioned that in CKN the conductivity relaxation times evaluated from  $M''$  at high temperatures closely follow the  $\alpha$ -relaxation times obtained from mechanical exper-

iments [44]. In addition, modulus spectra in ionically conducting glass-formers closely resemble the loss spectra of non-conducting molecular glass-formers as demonstrated in Fig. 4 for CKN (compare to Fig. 2(b)). Prominent asymmetrically shaped  $\alpha$ -peaks show up strongly shifting through the frequency window with temperature. There are also some indications for an excess wing, however less well pronounced than, e.g., in glycerol (Fig. 2(b)), but this may be partly due to the lower resolution of the measurements. At high frequencies in the GHz range a minimum is observed, exhibiting quite similar characteristics as the  $\epsilon''(\nu)$  minimum of glycerol. Also for CKN, the minimum region reveals clear indications for additional contributions due to a fast dynamic process [11,35].

In the following we will discuss the results on  $\alpha$ -relaxation and excess wing in some more detail. For a detailed discussion of the high-frequency response, including minimum and boson peak the reader is referred to earlier work from our and other groups [10,11,13,14, 23,25,37,47,51,52].

#### 4.2. The $\alpha$ -relaxation

The  $\alpha$ -peaks in both, glycerol (Fig. 2(b)) and CKN (Fig. 4), show marked deviations from Debye behavior, which is predicted for monodisper-

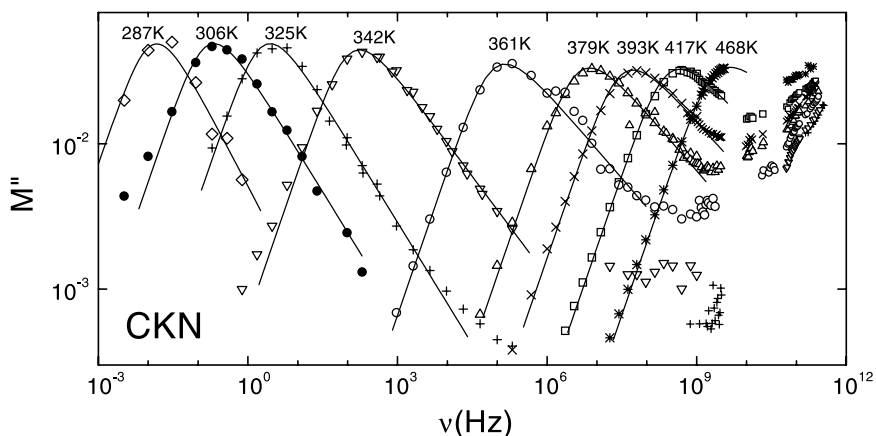


Fig. 4. Imaginary part of the dielectric modulus of CKN for various temperatures [35,44]. The lines are fits of the  $\alpha$ -peaks with the CD function.



sive exponential relaxation processes. This can be directly inferred from their significant asymmetry and their width being larger than the Debye value of 1.14. For the description of the  $\alpha$ -peak usually empirical functions are employed. In glass-forming materials, the Cole–Davidson (CD) function [57] is often used, which for the complex dielectric permittivity  $\varepsilon^*$  is given by

$$\varepsilon^* = \varepsilon_\infty + \frac{\varepsilon_s - \varepsilon_\infty}{(1 + i2\pi\nu\tau)^{\beta_{CD}}}. \quad (1)$$

Here  $\varepsilon_s$  and  $\varepsilon_\infty$  are the low and high frequency limits of the dielectric constant and  $\beta_{CD}$  is a width parameter. For  $\nu \gg \nu_p$  the loss calculated from Eq. (1) follows a power law with an exponent equal to  $-\beta_{CD}$ . For  $\beta_{CD} = 1$  the Debye response is recovered. As shown by the solid lines in Figs. 2 and 4, for glycerol and CKN good fits of the experimental data are possible with Eq. (1). Alternatively, often also the Fourier transform of a stretched-exponential decay is employed, but in glycerol and CKN and also in other glass-forming materials investigated by us, those fits are of somewhat lower quality [10,35,45,47]. However, various theoretical models for the relaxational dynamics of glass-forming materials indeed predict a shape of the  $\alpha$ -peaks similar to that of a KWW response [58].

As the broadening of the experimentally observed  $\alpha$ -peaks can be ascribed to a distribution of (Debye-) relaxation times, an average relaxation time can be calculated, which for the CD function is given by  $\langle\tau\rangle = \beta_{CD}\tau_{CD}$ . The corresponding relaxation rate,  $\nu_\tau = 1/(2\pi\langle\tau\rangle)$ , is virtually identical to the peak frequency  $\nu_p$ . In Figs. 5 and 6 we show  $\nu_p(T)$  for glycerol and CKN, respectively. As commonly found for most glass-forming liquids, for both materials the  $\nu_\tau(T)$  curves deviate significantly from thermally activated behavior leading to a pronounced curvature in the Arrhenius representations of Figs. 5 and 6. In addition for CKN at  $T_g$  a clear break in slope of the  $\nu_\tau(T)$  curve shows up (Fig. 6). Below  $T_g$  the mobile ions move in an environment essentially frozen on the time-scale of the experiment, leading to a temperature-independent mean activation energy. But also close to  $T_g$  a decoupling of the detected ionic motion and the structural  $\alpha$ -relaxation can be stated:

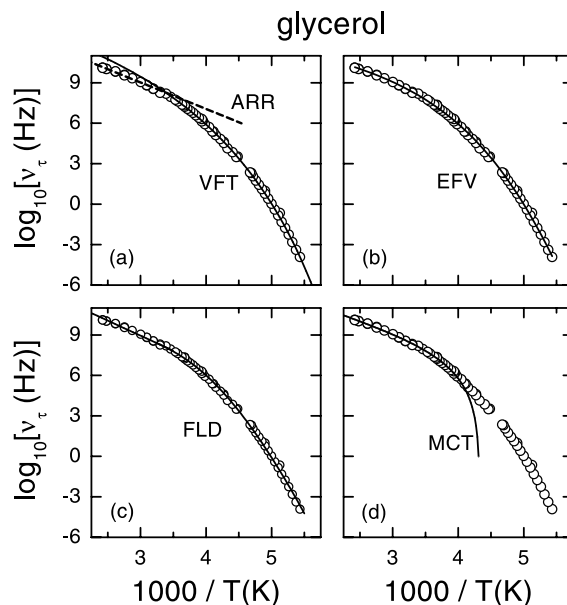


Fig. 5. Temperature dependence (Arrhenius representation) of the  $\alpha$ -relaxation rate of glycerol as determined from simultaneous fits of  $\varepsilon'(v)$  and  $\varepsilon''(v)$  with the CD-function (Fig. 2) [35]: (a) solid line: fit for  $T < 285$  K with VFT behavior [Eq. (2)], dashed line: high-temperature Arrhenius behavior; (b) fit with EFV theory; (c) fit with FLD theory; (d) fit for  $T > 280$  K with idealized MCT. Information on the fit parameters can be found in [35].

Here  $\nu_\tau$  is not equal to about  $10^{-3}$  Hz as would be expected from the usual definition of  $T_g$  by the relation  $\tau(T_g) = 100$  s [44]. For both materials at  $T > T_g$ , as in most glass formers,  $\nu_\tau(T)$  can be parameterized using the Vogel–Fulcher–Tammann (VFT) equation (Figs. 5(a) and 6(a)) [59]:

$$\nu_\tau = \nu_0 \exp \left[ \frac{-DT_{VF}}{T - T_{VF}} \right] \quad (2)$$

with  $T_{VF} = 124$  K for glycerol and 289 K for CKN [35]. The VFT law has a theoretical foundation in various theoretical models, e.g., the Adam–Gibbs theory [58,60] and the free volume theory [61,62]. Some high-temperature deviations from VFT behavior show up in glycerol, as observed in other glass-formers too and a transition to Arrhenius behavior may be suspected (dashed line) [63,64]. The transition temperature was sometimes interpreted as temperature, below which the potential energy landscape becomes important. In the

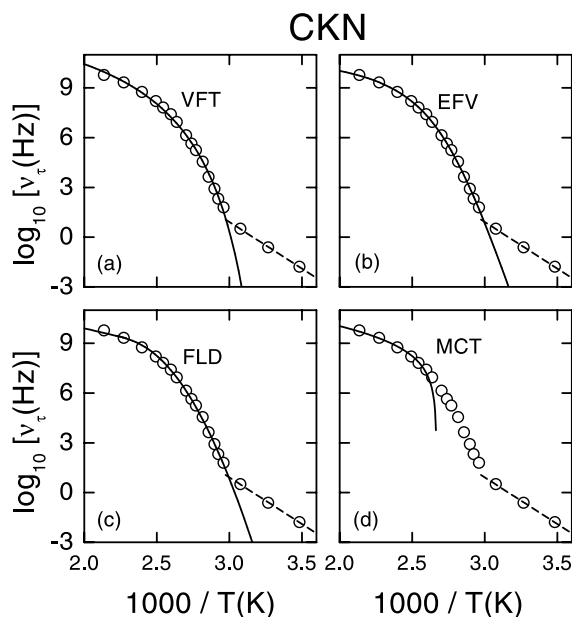


Fig. 6. Temperature dependence (Arrhenius representation) of the  $\alpha$ -relaxation rate of CKN as determined from fits of  $M''(\nu)$  with the CD-function (Fig. 4): (a) solid line: fit for  $T > 330$  K with VFT behavior [Eq. (2)]; (b) solid line: fit with EFV theory; (c) solid line: fit with FLD theory; (d) solid line: fit for  $T > 390$  K with MCT. The dashed lines in (a)–(d) show a fit with thermally activated behavior at  $T < T_g$ . Information on the fit parameters can be found in [35].

(b)–(d) parts of Figs. 5 and 6 we perform an analysis analogous to that presented earlier for glass-forming propylene carbonate (PC) in [47], fitting the experimental data to three different theoretical predictions. The models under consideration are the extended free volume (EFV) theory [62], the frustration-limited domain (FLD) theory [26,65] and the MCT, in its simplest version, the so-called idealized MCT [38,39]. For a brief discussion of the physical background of these theories the reader is referred to [47]; detailed information can be found in the references given above. Similar to our findings for PC, both EFV and FLD theory lead to fits of comparable quality. The MCT is able to describe the experimental data at high temperatures only, a behavior that can be understood within extended MCT, considering thermally activated hopping processes becoming important at low temperatures [38,39].

In Fig. 7(a) the width parameter of glycerol is plotted. A value  $\beta_{CD} = 1$  would imply a single relaxation time for all molecules. At high temperatures  $\beta_{CD}(T)$  tends to saturate at a value below unity. This is in contrast to the plausible notion that deep in the liquid state, due to the fast thermal fluctuations, each relaxing entity “sees” the same environment, leading to a mono-dispersive response. In CKN the width parameter of the modulus peaks even decreases with temperature [35]. The relaxation strength  $\Delta\epsilon$  of glycerol increases with decreasing temperature (Fig. 7(b)).  $\Delta\epsilon$ , determined by dielectric spectroscopy of dipolar materials is often affected by dipolar interactions. Usually the dipolar interactions lead to a strong increase of  $\Delta\epsilon$  with decreasing temperature, characterized by a Curie behavior,  $\Delta\epsilon \sim 1/T$ , which can be explained in the framework of the Onsager theory [66]. However for glycerol  $\Delta\epsilon(T)$  can be parameterized by a Curie–Weiss-like temperature dependence with a characteristic temperature of 97 K but also other descriptions may be possible. In CKN the amplitude of the modulus peaks is nearly constant [35].

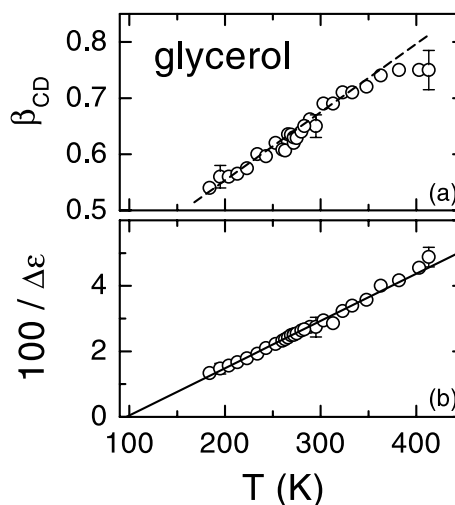


Fig. 7. Temperature dependence of  $\beta_{CD}$  (a) and  $100/\Delta\epsilon$  (b) of glycerol as determined from simultaneous fits of  $\epsilon'(\nu)$  and  $\epsilon''(\nu)$  with the CD-function (Fig. 2). The dashed line in (a) is drawn to guide the eye. The solid line in (b) represents a Curie–Weiss law.

### 4.3. The excess wing

As mentioned above, in the  $\varepsilon''(\nu)$  spectra of glycerol (Fig. 2(b)) and other molecular glass formers [3,6,20–22] a well-pronounced excess wing shows up. The question arises if a corresponding feature can also be seen in the modulus spectra of ionically conducting glass formers. In CKN indeed a weak excess wing can be suspected, especially in the 325 K curve in Fig. 4. However its significance is low, the curve being restricted to frequencies <200 kHz due to the limited resolution of the measuring devices available to us at the time of measurement [44]. In Fig. 8 we show modulus spectra in  $[\text{Mg}(\text{NO}_3)_2]_{0.44}[\text{KNO}_3]_{0.56}$  (MKN) [67], which have been measured with better resolution, extending up to 200 MHz also for low temperatures. Indeed, especially for 338 K a well-developed excess wing is observed (dashed line).

As mentioned above, it is suggestive to assume that the excess wing is simply the high-frequency flank of a  $\beta$ -relaxation peak that itself is submerged under the much stronger  $\alpha$ -peak [12]. Of course  $\alpha$ -peak and excess wing can always formally be fitted by a sum of two relaxation peaks [3,31–33,35,68]. However, such fits cannot *prove* that a relaxation process causes the excess wing. An experimental proof for a second relaxation can only be provided by the detection of a shoulder or even a second peak in the loss spectra. It is a well-established experimental fact that in materials with

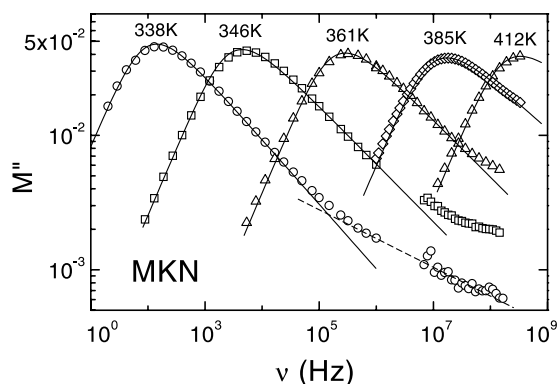


Fig. 8. Imaginary part of the dielectric modulus of MKN for various temperatures [67]. The lines are fits of the  $\alpha$ -peaks with the CD function. The dashed line indicates the excess wing.

well-resolved  $\beta$ -relaxation, its time scale successively separates from that of the  $\alpha$ -relaxation with decreasing temperature. However, in glass formers without a well-resolved  $\beta$ -peak, very low temperatures, below  $T_g$ , may be necessary to actually observe this separation. But below  $T_g$ , aging effects start to play a role. Aging occurs when the sample has fallen out of thermodynamic equilibrium, i.e. simply spoken, after cooling, the molecules move so slowly that they do not reach a new equilibrium position during reasonable observation times. Therefore in those materials, only after very long aging times below  $T_g$  the  $\alpha$ -peak may have shifted to sufficiently low frequencies for a  $\beta$ -peak to become visible. In Fig. 9 loss spectra for glycerol and two other molecular glass-formers, propylene carbonate (PC,  $T_g \approx 159$  K) and propylene glycol (PG,  $T_g \approx 168$  K), are shown at a temperature somewhat below  $T_g$  for different times after reaching this temperature [12,68]. For glycerol the curve after maximum aging time is also shown in Fig. 2(b). The frequency range of Fig. 9 was chosen to cover the excess wing region only. The  $\alpha$ -peak is located at very low frequencies and in  $\varepsilon''(\nu)$  is manifested in the somewhat steeper increase towards low frequencies. In Fig. 9, for all materials the typical power law, characteristic of an excess wing, shows up for short aging times. During aging, when thermodynamic equilibrium is being approached, the  $\alpha$ -peak can be assumed to shift towards lower frequencies, which can be understood within the concept of the fictive temperature [69]. This will lead to an increasing separation of  $\alpha$ - and  $\beta$ -peak and the presence of a  $\beta$ -peak may become more clearly visible. Indeed, as can be seen in Fig. 9, after the maximum aging times of up to five weeks for glycerol and PC and 6.5 d for PG, the excess wing has developed into a shoulder! (For a consideration of the significance of the, especially for glycerol (Fig. 9(a)), somewhat subtle curvature in  $\varepsilon''(\nu)$  the reader is referred to [12,70].) This behavior found for the three materials shown in Fig. 9 and for Salol [70] so far, strongly supports the assumption that a  $\beta$ -relaxation is responsible for the excess wing in glass-forming materials.

As mentioned already, fits using the sum of two relaxation peaks to describe  $\alpha$ -peak and excess wing can always be successfully performed. It is

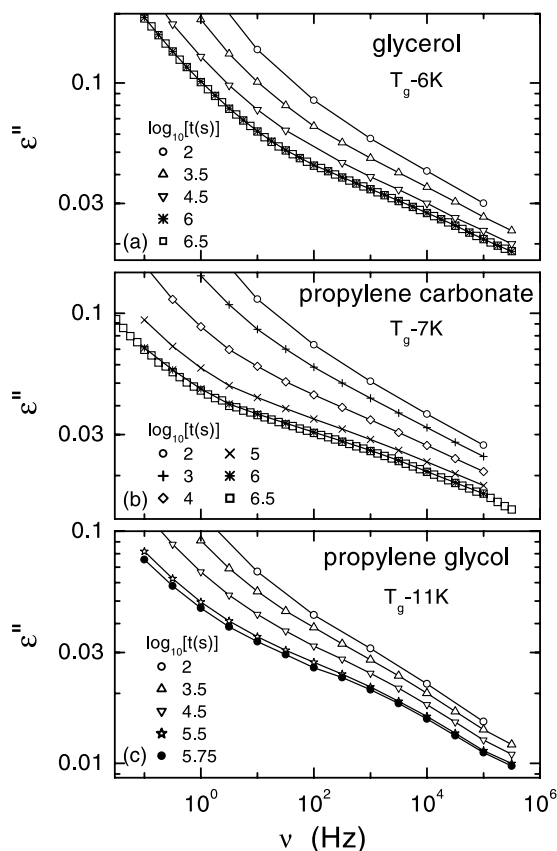


Fig. 9. Frequency-dependent dielectric loss of glycerol, propylene carbonate, and propylene glycol for different aging times  $t$  (not all shown) [12,68]. The lines are drawn to guide the eyes. After maximum aging times of about five weeks, the spectra in PC and glycerol have been collected for an extended number of frequencies.

clear that as long as a curvature in the excess wing region is seen, i.e. as long as the submerged  $\beta$ -peak is sufficiently separated from the  $\alpha$ -peak to show up as a shoulder or even peak, significant information can be gained about the parameters of the  $\beta$ -relaxation, e.g., relaxation time or peak width. However, the question arises if this is also the case for spectra where the  $\beta$ -peak is so close to the  $\alpha$ -peak and/or of so low amplitude, that only its high-frequency power law remains visible showing up as typical excess wing. This scenario is valid in the typical excess wing materials as glycerol and it would be highly desirable to learn more about the properties of the  $\beta$ -process in this class of materials

(“type A” in [28]) and to compare these to the well-known properties of the Johari–Goldstein-processes in glass-formers with well-pronounced  $\beta$ -peaks (“type B”). In Fig. 10, for the 213 K loss-curve of glycerol, we show a fit (solid line), which is composed of a simple additive superposition of a CD function for the  $\alpha$ -peak (dash-dotted line) and a Cole–Cole function for the  $\beta$ -peak (dashed line). The Cole–Cole function [71] was chosen, as it is able to fit the  $\beta$ -peaks in most type B glass-formers. Similar descriptions are possible also for the results at different temperatures and also for the other materials [35,68,72]. In the inset, displaying the excess-wing region in the same scaling as the main frame, a fit is shown with  $\tau_\beta$  fixed  $1 \times 10^{-8}$  s, eight times lower than  $\tau_\beta$  obtained from the best fit. It is not possible to achieve a reasonable agreement with the experimental data in this way. The fixed lower value of  $\tau_\beta$  leads to a stronger separation of  $\alpha$ - and  $\beta$ -peak and a pronounced shoulder in the fit curve arises, which is not found in the measured data. While it is clear that there is quite a lot of freedom in shifting the  $\beta$ -peak towards lower frequencies (then only its high-frequency wing is “used” for the fits), it cannot be indefinitely shifted to high frequencies, i.e. it is possible to at least extract a lower limit for  $\tau_\beta$  from fits of the kind shown in Fig. 10.

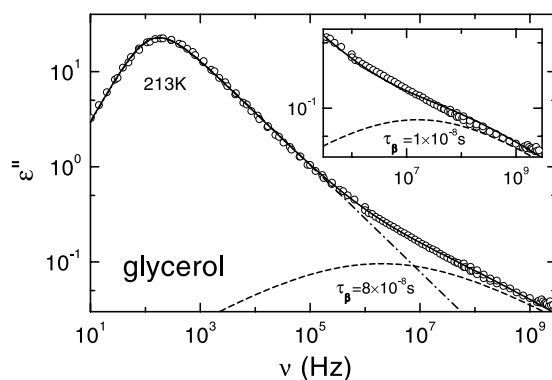


Fig. 10. Frequency-dependent dielectric loss of glycerol at 213 K. The solid line is a fit with the sum of a Cole–Davidson (dash-dotted line) and a Cole–Cole function (dotted line). In the inset the excess-wing region is shown, with a fit where  $\tau_\beta$  was fixed to an eight times lower value than in the fit of the main frame.

In Fig. 11 the temperature dependence of the  $\alpha$ -relaxation time of glycerol is shown, together with the  $\beta$ -relaxation times obtained in a similar way as demonstrated in Fig. 10 [35,73]. The error bars indicate the lower limit of  $\tau_\beta$  as explained above. These results and those in other type A glass-formers [35,68] reveal a  $\beta$ -relaxation time that shows significant deviations from Arrhenius behavior. Taking into account the error bars, it is not possible to describe the experimental data by fixing the values of  $\tau_\beta(T)$  to a thermally activated Arrhenius behavior. This detection of a non-Arrhenius  $\tau_\beta(T)$  is astonishing as the  $\beta$ -relaxation times, determined in type B glass-formers are believed to follow an Arrhenius behavior. Thus one may have objections to using the term “ $\beta$ -relaxation” for the relaxation causing the excess wing. In fact it could be possible that there are two different kinds of relaxations beyond the  $\alpha$ -relaxation, which both are inherent to glass-forming matter [74]: the Johari–Goldstein  $\beta$ -relaxation and the relaxation causing the excess wing, both having different microscopic origins. From an experimental point of view it is difficult to decide whether or not this

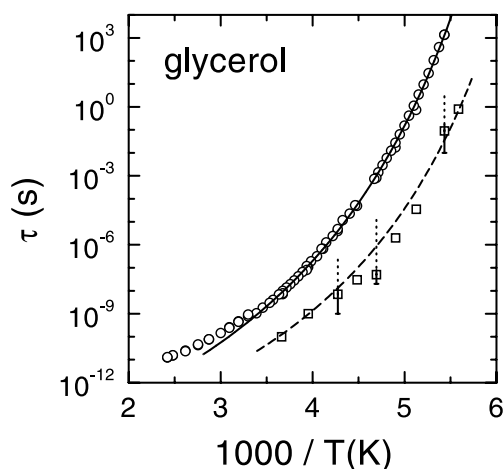


Fig. 11. Temperature-dependent  $\alpha$ -relaxation time (circles) and  $\beta$ -relaxation time (squares) as determined from fits as shown in Fig. 10. The partly dashed error bars indicate that only a lower limit for  $\tau_\beta$  can be deduced from the fits. The solid line is a fit for  $T < 285$  K with VFT behavior (cf. Fig. 5(a)). The dashed line demonstrates VFT behavior also for  $\tau_\beta(T)$ , using the same  $\tau_0$  and  $T_{VF}$  as for  $\tau_\alpha(T)$ , however alternative descriptions may be possible.

relaxation and the Johari–Goldstein  $\beta$ -relaxations observed in type B glass formers originate from the same microscopic process.

However, it should be remarked that there is no principal reason that the  $\beta$ -process dynamics should always show Arrhenius behavior, especially as its microscopic origin can be regarded as unclarified yet. If the excess wing is indeed due to a  $\beta$ -relaxation, the difference between type B and type A glass formers may be caused just by the temperature evolution of the  $\beta$ -dynamics: In the first materials it is rather weak, presumably Arrhenius, leading to a clear separation of both relaxation times at low temperatures which thus enables a clear detection of the  $\beta$ -peak. In contrast, in the latter materials the relaxation time of the  $\beta$ -process may more closely follow that of the  $\alpha$ -process (which is non-Arrhenius) and only the high-frequency flank of the  $\beta$ -peak, the excess wing, is visible (except at low temperatures after aging). Such an uncommon temperature dependence of  $\tau_\beta$  was already suspected by Johari and Goldstein to explain the apparent absence of a  $\beta$ -relaxation in some glass-formers [2]. In addition, this scenario seems to be consistent with the recently found correlation of  $\tau_\beta(T_g)$  and the Kohlrausch-exponent  $\beta_{KWW}(T_g)$  describing the width of the  $\alpha$ -peak [75] as discussed in detail in [68]. Finally it should be mentioned that in [6] it was shown that it is possible to collapse dielectric spectra of various type A glass formers, collected at different temperatures, onto one master curve by an appropriate scaling of the axes. The implications of this scaling behavior in light of the explanation of the excess wing by a  $\beta$ -relaxation, promoted in the present work, are discussed in [12,70].

## 5. Summary and Conclusion

In the present work, broadband dielectric spectra of several prototypical glass-formers, belonging to the group of dipolar molecular and ionically conducting glass-formers, have been presented thereby giving an overview over the rich kinetic behavior of glass-forming systems. In the dielectric-loss spectra of molecular glass formers, as shown here for glycerol, four different contri-

contributions can be clearly distinguished: the  $\alpha$ -peak, the excess wing, the minimum, and the boson peak. Plotting the dielectric modulus spectra for ionically conducting glass-formers (here CKN) the same contributions seem to be present, too. These spectral features can be attributed to four distinct kinetic processes that seem to hallmark glassy dynamics in general:

1. The  $\alpha$ -relaxation, with its tremendous continuous slow down when approaching  $T_g$  from the liquid state, thereby clearly deviating from Arrhenius behavior. The spectral shape of the  $\alpha$ -peaks reveals marked deviations from single-exponential relaxation, which nowadays is commonly attributed to microscopic heterogeneity effects [15].
2. The  $\beta$ -relaxation, causing either a well-defined peak or shoulder or an excess wing, depending on its closeness to the  $\alpha$ -peak. It is suggestive that the  $\beta$ -relaxations causing the excess wing and the Johari–Goldstein relaxations observed in type B glass-formers mirror the same kinetic process that may be present in all glass-forming materials.
3. The fast process showing up as an excess contribution in the minimum region of  $\varepsilon''(\nu)$  or  $M''(\nu)$  at GHz–THz frequencies.
4. The process leading to the boson peak, marking fast, presumably phonon-like dynamics.

A large variety of competing microscopic explanations of these processes has appeared during recent years. None of those can take account of the complete, very rich kinetics observed in glass-forming materials, involving all four processes and extending from the liquid well into the glassy state. Consensus seems to emerge that MCT provides a correct picture of the dynamic processes at high temperatures, in the liquid and supercooled liquid state. But much work still has to be done, e.g., to achieve an understanding of the Johari–Goldstein  $\beta$ -relaxations that separate from the  $\alpha$ -relaxation at low temperatures. The recent tremendous theoretical and experimental activity in the field of glass physics gives rise to the hope that the many open questions will be solved in due course, finally arriving at a consistent picture of the glass transition and dynamics in near future.

## Acknowledgements

We thank R. Brand, M. Dressel, Yu.G. Goncharov, B. Gorshunov, A. Pimenov, and U. Schneider for their contributions to the dielectric measurements. We are obliged to A. Maiazza for the preparation of the CKN samples and to Th. Wiedenmann for technical support. This work was supported by the DFG, Grant-No. LO264/8-1 and partly by the BMBF, Contract-No. EKM 13N6917.

## References

- [1] F.S. Howell, R.A. Bose, P.B. Macedo, C.T. Moynihan, *J. Phys. Chem.* 78 (1974) 639.
- [2] G.P. Johari, M. Goldstein, *J. Chem. Phys.* 53 (1970) 2372.
- [3] A. Hofmann, F. Kremer, E.W. Fischer, A. Schönhal, in: R. Richert, A. Blumen (Eds.), *Disorder Effects on Relaxational Processes*, Springer, Berlin, 1994, p. 309.
- [4] K. Funke, *Philos. Mag. A* 68 (1993) 711.
- [5] K.L. Ngai, C. Cramer, T. Saatkamp, K. Funke, in: M. Giordano, et al. (Eds.), *Proceedings of the Workshop on Non-Equilibrium Phenomena in Supercooled Fluids, Glasses, and Amorphous Materials*, Pisa, Italy, 1995, World Scientific, Singapore, 1996, p. 3.
- [6] P.K. Dixon, L. Wu, S.R. Nagel, B.D. Williams, J.P. Carini, *Phys. Rev. Lett.* 65 (1990) 1108.
- [7] A. Schönhal, F. Kremer, E. Schlosser, *Phys. Rev. Lett.* 67 (1991) 999.
- [8] M. Arndt, R. Stannarius, H. Groothues, E. Hempel, F. Kremer, *Phys. Rev. Lett.* 79 (1997) 2077.
- [9] B. Schiener, R. Böhmer, A. Loidl, R.V. Chamberlin, *Science* 274 (1996) 752.
- [10] P. Lunkenheimer, A. Pimenov, M. Dressel, Yu.G. Goncharov, R. Böhmer, A. Loidl, *Phys. Rev. Lett.* 77 (1996) 318.
- [11] P. Lunkenheimer, A. Pimenov, A. Loidl, *Phys. Rev. Lett.* 78 (1997) 2995.
- [12] U. Schneider, R. Brand, P. Lunkenheimer, A. Loidl, *Phys. Rev. Lett.* 84 (2000) 5560.
- [13] P. Lunkenheimer, U. Schneider, R. Brand, A. Loidl, *Contemp. Phys.* 41 (2000) 15.
- [14] P. Lunkenheimer, A. Loidl, in: F. Kremer (Ed.), *Broadband Dielectric Spectroscopy*, Springer, Berlin (in press).
- [15] For reviews on heterogeneity in glass-forming liquids, see: H. Sillescu, *J. Non-Cryst. Solids* 243 (1999) 81; M.D. Ediger, *Annu. Rev. Phys. Chem.* 51 (2000) 99.
- [16] S.R. Elliott, *Philos. Mag. B* 60 (1989) 777; S.R. Elliott, *J. Non-Cryst. Solids* 116 (1990) 179.
- [17] K. Funke, *Solid State Ionics* 18/19 (1986) 183; K. Funke, J. Hermeling, J. Kümpers, *Z. Naturforsch. a* 43 (1988) 1094.

- [18] P.B. Macedo, C.T. Moynihan, R. Bose, *Phys. Chem. Glasses* 13 (1972) 171.
- [19] R.H. Cole, E. Tombari, *J. Non-Cryst. Solids* 131–133 (1991) 969;  
S.R. Elliott, *J. Non-Cryst. Solids* 170 (1994) 97;  
C.T. Moynihan, *J. Non-Cryst. Solids* 172–174 (1994) 1395;  
D.L. Sidebottom, P.F. Green, R.K. Brow, *J. Non-Cryst. Solids* 183 (1995);  
B. Roling, A. Happe, K. Funke, M.D. Ingram, *Phys. Rev. Lett.* 78 (1997) 2160;  
B. Roling, *J. Non-Cryst. Solids* 244 (1999) 34.
- [20] P. Lunkenheimer, A. Pimenov, B. Schiener, R. Böhmer, A. Loidl, *Europhys. Lett.* 33 (1996) 611.
- [21] R.L. Leheny, S.R. Nagel, *Europhys. Lett.* 39 (1997) 447.
- [22] A. Kudlik, S. Benkhof, T. Blochowicz, C. Tschirwitz, E. Rössler, *J. Mol. Struct.* 479 (1999) 201.
- [23] P. Lunkenheimer, U. Schneider, R. Brand, A. Loidl, in: M. Tokuyama, I. Oppenheim (Eds.), *Slow Dynamics in Complex Systems: Eighth Tohwa University International Symposium*, AIP Conference Proceedings No. 469, AIP, New York, 1999, p. 433.
- [24] R.V. Chamberlin, *Phys. Rev. B* 48 (1993) 15638.
- [25] R.V. Chamberlin, *Phys. Rev. Lett.* 82 (1999) 2520.
- [26] G. Tarjus, D. Kivelson, S. Kivelson, in: J.T. Fourkas, et al. (Eds.), *Supercooled Liquids, Advances and Novel Applications*, ACS Symposium Series, vol. 676, American Chemical Society, Washington, DC, 1997, p. 67.
- [27] G.P. Johari, in: M. Goldstein, R. Simha (Eds.), *The Glass Transition and the Nature of the Glassy State*, *Annals of the New York Academy of Sciences*, vol. 279, 1976, p. 117.
- [28] A. Kudlik, S. Benkhof, T. Blochowicz, C. Tschirwitz, E. Rössler, *J. Mol. Struct.* 479 (1999) 201.
- [29] While this classification is useful to quickly denote systems with clear excess wing or  $\beta$ -relaxation, however, one has to state clearly that it may be somewhat oversimplifying and that there certainly are examples that do not fit into this scheme.
- [30] N.B. Olsen, *J. Non-Cryst. Solids* 235–237 (1998) 399.
- [31] M. Jiménez-Ruiz, M.A. González, F.J. Bermejo, M.A. Miller, N.O. Birge, I. Cendoya, A. Alegría, *Phys. Rev. B* 59 (1999) 9155.
- [32] C. León, K.L. Ngai, *J. Phys. Chem. B* 103 (1999) 4045.
- [33] C. León, K.L. Ngai, C.M. Roland, *J. Chem. Phys.* 110 (1999) 11585.
- [34] H. Wagner, R. Richert, *J. Chem. Phys.* 110 (1999) 11660.
- [35] P. Lunkenheimer, *Dielectric Spectroscopy of Glassy Dynamics*, Shaker, Aachen, 1999.
- [36] J. Wuttke, J. Hernandez, G. Li, G. Coddens, H.Z. Cummins, F. Fujara, W. Petry, H. Sillescu, *Phys. Rev. Lett.* 72 (1994) 3052.
- [37] P. Lunkenheimer, A. Pimenov, M. Dressel, B. Gorshunov, U. Schneider, B. Schiener, A. Loidl, in: J.T. Fourkas, D. Kivelson, U. Mohanty, K.A. Nelson (Eds.), *Supercooled Liquids: Advances and Novel Applications*, ACS Publications, Washington, DC, 1997, p. 168.
- [38] U. Bengtzelius, W. Götze, A. Sjölander, *J. Phys. C* 17 (1984) 5915;  
W. Götze, L. Sjögren, *Rep. Progr. Phys.* 55 (1992) 241.
- [39] For reviews of MCT, see: W. Götze, L. Sjögren, *Rep. Progr. Phys.* 55 (1992) 241;  
E. Schilling, in: R. Richert, A. Blumen (Eds.), *Disorder Effects on Relaxational Properties*, Springer, Berlin, 1994, p. 193;  
H.Z. Cummins, *J. Phys.: Condes. Matter* 11 (1999) A95.
- [40] R. Böhmer, B. Schiener, J. Hemberger, R.V. Chamberlin, *Z. Phys.* 99 (1995) 91.
- [41] R. Böhmer, M. Maglione, P. Lunkenheimer, A. Loidl, *J. Appl. Phys.* 65 (1989) 901.
- [42] A.A. Volkov, Yu.G. Goncharov, G.V. Kozlov, S.P. Lebedev, A.M. Prokhorov, *Infrared Phys.* 25 (1985) 369;  
A.A. Volkov, G.V. Kozlov, S.P. Lebedev, A.M. Prokhorov, *Infrared Phys.* 29 (1989) 747.
- [43] U. Schneider, P. Lunkenheimer, A. Pimenov, R. Brand, A. Loidl, *Ferroelectrics* 249 (2001) 89.
- [44] A. Pimenov, P. Lunkenheimer, H. Rall, R. Kohlhaas, A. Loidl, R. Böhmer, *Phys. Rev. E* 54 (1996) 676.
- [45] U. Schneider, P. Lunkenheimer, R. Brand, A. Loidl, *J. Non-Cryst. Solids* 235–237 (1998) 173.
- [46] P. Lunkenheimer, U. Schneider, R. Brand, A. Loidl, *Phys. Bl.* 56 (2000) 35.
- [47] U. Schneider, P. Lunkenheimer, R. Brand, A. Loidl, *Phys. Rev. E* 59 (1999) 6924.
- [48] A. Schönhals, F. Kremer, A. Hofmann, E.W. Fischer, E. Schlosser, *Phys. Rev. Lett.* 70 (1993) 3459.
- [49] P.K. Dixon, N. Menon, S.R. Nagel, *Phys. Rev. E* 50 (1994) 1717.
- [50] M.D. Ediger, C.A. Angell, S.R. Nagel, *J. Phys. Chem* 100 (1996) 13200.
- [51] W. Götze, T. Voigtmann, *Phys. Rev. B* 61 (2000) 4133.
- [52] J. Wuttke, M. Ohl, M. Goldammer, S. Roth, U. Schneider, P. Lunkenheimer, R. Kahn, B. Rufflé, R. Lechner, M.A. Berg, *Phys. Rev. E* 61 (2000) 2730;  
M. Goldammer, C. Losert, J. Wuttke, W. Petry, F. Terki, H. Schober, P. Lunkenheimer, *Phys. Rev. E* 64 (2001) 021303.
- [53] J. Wong, C.A. Angell, *Glass: Structure by Spectroscopy*, Marcel Dekker, New York, 1976;  
U. Strom, J.R. Hendrickson, R.J. Wagner, P.C. Taylor, *Solid State Commun.* 15 (1974) 1871;  
U. Strom, P.C. Taylor, *Phys. Rev. B* 16 (1977) 5512;  
C. Liu, C.A. Angell, *J. Chem. Phys.* 93 (1990) 7378;  
R.H. Cole, E. Tombari, *J. Non-Cryst. Solids* 131–133 (1991) 969;  
T.S. Perova, J.K. Vij, *J. Mol. Liquids* 69 (1996) 1;  
T.S. Perova, J.K. Vij, D.H. Christensen, O.F. Nielsen, *J. Mol. Struct.* 479 (1999) 111.
- [54] J. Ross Macdonald, *Impedance Spectroscopy*, Wiley, New York, 1987.
- [55] A.K. Jonscher, *Dielectric Relaxations in Solids*, Chelsea Dielectrics Press, London, 1983.
- [56] W.K. Lee, J.F. Liu, A.S. Nowick, *Phys. Rev. Lett.* 67 (1991) 1559;

- S.R. Elliott, *Solid State Ionics* 70/71 (1994) 27;  
D.L. Sidebottom, P.F. Green, R.K. Brow, *Phys. Rev. Lett.* 74 (1995) 5068.
- [57] D.W. Davidson, R.H. Cole, *J. Chem. Phys.* 18 (1950) 1417;  
D.W. Davidson, R.H. Cole, *J. Chem. Phys.* 19 (1951) 1484.
- [58] For a review of various theories of the glass transition, see:  
J. Jäckle, *Rep. Prog. Phys.* 49 (1986) 171.
- [59] H. Vogel, *Phys. Z.* 22 (1921) 645;  
G.S. Fulcher, *J. Am. Ceram. Soc.* 8 (1923) 339;  
G. Tammann, W. Hesse, *Z. Anorg. Allg. Chem.* 156 (1926) 245.
- [60] G. Adam, J.H. Gibbs, *J. Chem. Phys.* 43 (1965) 139.
- [61] M.H. Cohen, D. Turnbull, *J. Chem. Phys.* 31 (1959) 1164.
- [62] M.H. Cohen, G.S. Grest, *Phys. Rev. B* 20 (1979) 1077;  
G.S. Grest, M.H. Cohen, *Adv. Chem. Phys.* 48 (1981) 455.
- [63] F. Stickel, E.W. Fischer, R. Richert, *J. Chem. Phys.* 104 (1996) 2043.
- [64] F. Stickel, E.W. Fischer, R. Richert, *J. Chem. Phys.* 102 (1995) 6251.
- [65] D. Kivelson, S.A. Kivelson, X.-L. Zhao, Z. Nussinov, G. Tarjus, *Physica A* 219 (1995) 27.
- [66] H. Fröhlich, in: *Theory of Dielectrics*, Oxford University Press, London, 1950, p. 33.
- [67] A. Pimenov, P. Lunkenheimer, M. Nicklas, R. Böhmer, A. Loidl, C.A. Angell, *J. Non-Cryst. Solids* 220 (1997) 93.
- [68] K.L. Ngai, P. Lunkenheimer, C. León, U. Schneider, R. Brand, A. Loidl, *J. Chem. Phys.* 115 (2001) 1405.
- [69] see, e.g.: C.T. Moynihan et al., *Ann. New York Acad. Sci.* 279 (1976) 15.
- [70] P. Lunkenheimer, R. Wehn, Th. Riegger, A. Loidl, *J. Non-Cryst. Solids* (in press).
- [71] K.S. Cole, R.H. Cole, *J. Chem. Phys.* 9 (1941) 341.
- [72] P. Lunkenheimer, A. Loidl, *Dynamic processes at the glass transition*, in: B. Kramer (Ed.), *Advances in Solid State Physics*, vol. 41, Springer, Berlin, 2001, p. 405.
- [73] To take into account a possible influence from the fast process prevailing in the  $\varepsilon''(\omega)$ -minimum region, the fits have been performed including a phenomenological description of the minimum region [23,35]. Only slightly different values of  $\tau_\beta$ , compared to the procedure demonstrated in Fig. 10, are obtained.
- [74] E. Rössler, private communication.
- [75] K.L. Ngai, *Phys. Rev. E* 57 (1998) 7346.